Performance of fourier domain vs. time domain optical coherence tomography

R. Leitgeb, C. K. Hitzenberger, and A. F. Fercher

Department of Medical Physics, University of Vienna, Waehringerstr. 13, A-1090 Vienna, Austria

Rainer.Leitgeb@unvie.ac.at

http://www.univie.ac.at/meph/lambda

Abstract: In this article we present a detailed discussion of noise sources in Fourier Domain Optical Coherence Tomography (FDOCT) setups. The performance of FDOCT with charge coupled device (CCD) cameras is compared to current standard time domain OCT systems. We describe how to measure sensitivity in the case of FDOCT and confirm the theoretically obtained values. It is shown that FDOCT systems have a large sensitivity advantage and allow for sensitivities well above 80dB, even in situations with low light levels and high speed detection.

OCIS codes: (110.4500) Optical Coherence Tomography, (120.3890) Medical optics instrumentation

References and links

1. A. F. Fercher, C. K. Hitzenberger, G. Kamp, S.Y. El-Zaiat, "Measurement of intraocular distances by backscattering spectral interferometry," Opt.Commun. **117**, 43-48,(1995).
2. G. Häusler, M.W. Lindner, "Coherence radar and spectral radar – new tools for dermatological diagnosis," J. Biomed. Opt. **3,** 21-31(1998).
3. M. Wojtkowski, R. Leitgeb, A. Kowalczyk, T. Bajraszewski, A. F. Fercher ,"In vivo human retinal imaging by fourier domain optical coherence tomography," J. Biomed. Opt. **7**, 457-463 (2002).
4. M. Wojtkowski, T. Bajraszewski, P. Targowski, A. Kowalczyk, "Real-time in-vivo ophthalmic imaging by ultrafast spectral interferometry," Proc. SPIE 4956, 4956-11 (2003).
5. J. W. Goodman, *Statistical Optics* (John Wiley & Sons, 1985).
6. R. V. Sorin, D. M. Baney, "A simple intensity noise reduction technique for optical low coherence reflectometry," IEEE Photonics Techn. Lett. 4, 1404 – 1406, (1992).
7. A. M. Rollins, J. A. Izatt, "Optimal interferometer designs for optical coherence tomography," Opt. Lett. **24**, 1484-1486 (1999).
8. A. G. Podoleanou, "Unbalanced versus balanced operation in an optical coherence tomography system," Appl. Opt. **39**, 173-182 (2000).
9. H. Saint-Jalmes, M. Lebec, E. Beaurepierre, A. Dubois, A. C. Boccara, in *Handbook of Optical Coherence Tomography* , B. Bouma, E. Tearney, eds.,(Marcel Dekker, Inc. 2002) Chap.11.
10. R. Bracewell, *The Fourier Transform and Its Applications*, (McGraw-Hill 1965).
11. A. M. Rollins, S. Yazdanfar, M. D. Kulkarni, R. Ung-Arunyawee, J. A. Izatt," In vivo video rate optical coherence tomography,*"* Opt. Express **3,** 219-229 (1998), http://www.opticsexpress.org/abstract.cfm?URI=OPEX-3-6-219.
12. R. Leitgeb, L. Schmetterer, C. K. Hitzenberger, M. Sticker, M. Wojtkowski, and A. F. Fercher," Flow Measurements by Frequency Domain Optical Coherence Tomography," Proc. SPIE **4619**, 16-21 (2002).

Ever since the first medical applications of Fourier Domain Optical Coherence Tomography (FDOCT) have been described by Fercher *et al.* in 1995[1], it has been questioned if this technique is competitive to current standard time domain systems. Whereas Time Domain OCT (TDOCT) is already well established and finds a still growing field of applications in medical diagnostics, it is only a couple of years ago that first FDOCT in-vivo images have been presented[2,3]. Recent results demonstrated that even in small signal power situations the

#2241 - $15.00 US Received March 17, 2003; Revised April 09, 2003

system was able to reveal anatomic structures and their dynamics on the ocular fundus[4]. This paper is devoted to a detailed discussion of noise sources in FDOCT systems in direct comparison to TDOCT.

In FDOCT setups optical energy is measured rather than optical power. This is due to the fact that CCD detectors collect photoelectron charges during the exposure time τ whereas PIN detectors register the continuous photoelectron current $i_e(t)$. The number of photoelectrons n_e, and the photoelectron current are related to the optical power P as $n_e = \eta P \tau / h\nu_0$, and $i_e = \eta P q_e / h\nu_0$ where η denotes the detector quantum efficiency, h is the Planck constant, ν_0 is the center frequency of the light source spectrum, and q_e is the electron charge. The interference pattern is recorded by a spectrometer as a function of frequency rather than time. The object structure is obtained from the interference pattern by a discrete Fourier transform (DFT)[1].

Assume two mirrors with reflectivity R_s and R_r in the sample and reference arm of a Michelson interferometer. Let the part of the input power that will exit the interferometer from each arm be γ_r and γ_s respectively, assuming R_s=R_r=1. We have a fixed photon charge distribution $K(n)$ over the detector pixel array of the spectrometer. For each read out cycle with exposure time τ it is given by

$$K(n) = \frac{\rho\eta\tau}{h\nu_n} \cdot P(\nu_n)\left[\gamma_s R_s + \gamma_r R_r + 2\sqrt{\gamma_r \gamma_s R_r R_s}\cos(4\pi\nu_n \Delta z / c + \varphi)\right], \quad n = 0,\ldots,N-1 \quad , \qquad (1)$$

where $P(\nu_n)$ is the spectral optical power at the interferometer entrance , and N determines the number of pixels. The spectrometer efficiency ρ comprises the diffraction grating efficiency and losses due to optical components and spectrometer geometry. The optical path length difference between the two interferometer arms is Δz, and ϕ denotes an arbitrary phase shift. We assume a Gaussian spectral density of the light source

$$P(\nu_n) = P(\nu_0)\exp\left[-\left(\frac{2\sqrt{\ln 2}(\nu_n - \nu_0)}{\Delta\nu_{FWHM}}\right)^2\right]. \qquad (2)$$

The n^{th} detector pixel covers a spectral range of $\nu_n \pm \delta\nu/2$, where $\delta\nu$ is the spectrometer resolution. Assuming, that the full width half maximum (FWHM) of the source spectrum is imaged onto N/m detector pixels, the resolution is given by $\delta\nu = \Delta\nu_{FWHM}\ m/N$. In taking the integral over Eq. (2) one calculates the output power of the light source to be $P_0 = \sqrt{\pi/4\ln 2}\,\Delta\nu_{FWHM} P(\nu_0)$.

Table 1. Detector signals and noise sources for FD and TDOCT systems.

	Fourier Domain (FD)[5]	Time Domain (TD) [6,7,8]
Interference signal	$S(\nu_0)_{FDOCT} = \frac{\rho\eta\tau}{h\nu_0} 2P(\nu_0)\sqrt{\gamma_r\gamma_s R_r R_s}$	$\left\langle S_{TDOCT}{}^2 \right\rangle = 2S^2 P_0{}^2 \gamma_r\gamma_s R_r R_s$
DC signal S_{DC}	$\frac{\rho\eta\tau}{h\nu_0}\frac{P_0}{N}(\gamma_s R_s + \gamma_r R_r)$	$SP_0(\gamma_s R_s + \gamma_r R_r)$
$\sigma_{shot}{}^2$	$\frac{\rho\eta\tau}{h\nu_0}\frac{P_0}{N}(\gamma_s R_s + \gamma_r R_r)$	$2q_e SP_0(\gamma_s R_s + \gamma_r R_r)B$
$\sigma_{excess}{}^2$	$\frac{(1+\Pi^2)}{2}\left(\frac{\rho\eta}{h\nu_0}\right)^2 \tau \cdot \frac{P_0{}^2}{N^2}(\gamma_s R_s + \gamma_r R_r)^2 \frac{N}{\Delta\nu_{eff}}$	$\frac{(1+\Pi^2)}{\Delta\nu_{eff}} S^2 \cdot P_0{}^2(\gamma_s R_s + \gamma_r R_r)^2 B$
$\sigma_{receiver}{}^2$	$\sigma_{read}{}^2 + \sigma_{dark}{}^2$	$\mathrm{NEC}^2\ B$

#2241 - $15.00 US
Received March 17, 2003; Revised April 09, 2003

Table 1 shows the theoretical signals and noise variances for each detector element for either FD and TD OCT systems. B is the electronic detection bandwidth, *S* is the detector responsitivity $S=\eta q_e/h\nu_0$, Π is the degree of polarisation, $\Delta\nu_{eff}$, is the effective spectral line width[7], and NEC is the noise equivalent current in pA/√Hz. Note that in the case of FD photoelectrons are counted whereas in time domain the effective photocurrent is measured. The photoelectron and photocurrent noise variances in the respective domains are related via $\sigma_{TD}^2 = \sigma_{FD}^2 (q_e/\tau)^2$. The electronic bandwidth is related to the exposure time by[9] $B=1/2\tau$. In order to obtain the excess noise variance one needs to take into account that each detector pixel detects only the N^{th} part of the full spectrum across the entire array. Hence, the effective line width is reduced by the same factor. The CCD receiver noise consists of dark noise and read noise, i.e., $\sigma_{receiver}{}^2 = \sigma_{dark}{}^2 + \sigma_{read}{}^2$. The read noise contains the Johnson noise of the amplifier circuit and the quantisation noise of the ADC. In practice the quantization depth of the ADC will always be chosen such that the associated noise level is much smaller than the receiver Johnson noise.

Another important noise source is Flicker or 1/f noise. Due to heterodyne signal detection with frequencies usually well above 10 kHz 1/f noise can be neglected in the case of time domain OCT. Fourier domain systems record one full A-scan in parallel. For short exposure times (< 1ms) also in this case 1/f noise will be neglected.

The FDOCT signal is obtained by DFT of the modulated photon charge distribution (1). The relationships between the maximum of a fully sinusoidally modulated Gaussian envelope $P(\nu_0)$ and the signal peak height at the corresponding modulation frequency after DFT S_{Peak}, and between the corresponding FWHM values read[10]

$$P(\nu_0) \xrightarrow{DFT} S(\tau)_{Peak} = \sqrt{\frac{\pi}{4\ln 2}} \frac{\Delta\nu^{(n)}_{FWHM}}{2N} P(\nu_0) = \frac{P_0}{2N},$$

$$\Delta\nu^{(n)}_{FWHM} \xrightarrow{DFT} \Delta\tau^{(h)}_{FWHM} = \frac{4\ln 2}{\pi} \frac{N}{\Delta\nu^{(n)}_{FWHM}} \quad . \tag{3}$$

The indices (h) and (n) indicate, that the values stand for the associated number of Fourier harmonics and pixel respectively, in particular, $\Delta\nu^{(n)}_{FWHM} = N/m$. Hence, the FDOCT signal amplitude is obtained by combining Eqs. (1) and (3):

$$S(\tau)^{Peak}{}_{FDOCT} = \frac{\rho\eta\tau}{h\nu_0} \frac{P_0}{N} \sqrt{\gamma_r \gamma_s R_r R_s} \quad . \tag{4}$$

Immediately one observes the factor of *1/N*, which seems to favour TD systems. The situation dramatically changes if we take into account the Fourier transformation process. The noise rms of each pixel contributes to the noise level at one DFT bin. This effect would increase the noise level at the DFT bin by factor of √N as compared to the pixel noise rms. However, we have an additional normalization factor of 1/N due to the DFT[10]. We finally end up with the relation $\tilde{\sigma}^2 = \sigma^2 / N$ for white noise variances in the respective DFT spaces. Assuming that all noise contributions have a white noise characteristic, the total noise in FDOCT systems after the DFT is given by $\tilde{\sigma}^2{}_{noise} = \frac{1}{N}\sigma^2{}_{noise} = \frac{1}{N}\left(\sigma^2{}_{shot} + \sigma^2{}_{excess} + \sigma^2{}_{receiver}\right)$.

The signal to noise ratio (SNR) is defined as $SNR = \left\langle S_{OCT}{}^2 \right\rangle / \sigma_{noise}{}^2$. In the case of FDOCT, $\sigma_{noise}{}^2$ has to be replaced by $\tilde{\sigma}_{noise}{}^2$, and S_{OCT} is given in Eq. (4). Since in Fourier domain setups the detector will always record the high DC background as well, the achievable dynamic range is limited by the photoelectron capacity (FWC) of the CCD. The sensitivity Σ of OCT devices is defined as the minimal sample arm reflectivity $R_{s,min}$, at which the SNR equals one, i.e., $\Sigma = 1/R_{s,min}$. In most applications the reference arm reflectivity is much larger

#2241 - $15.00 US Received March 17, 2003; Revised April 09, 2003

than that of the sample arm, i.e., $R_s << R_r$. Using this approximation the sensitivity may be written as

$$\Sigma_{FDOCT} = \frac{\frac{1}{N}\left(\frac{\rho\eta\tau}{h\nu_0}P_0\right)^2 \gamma_s\gamma_r R_r}{\frac{\rho\eta\tau}{h\nu_0}\cdot\frac{P_0}{N}\gamma_r R_r\left[1+\frac{\left(1+\Pi^2\right)}{2}\frac{\rho\eta}{h\nu_0}\cdot\frac{P_0}{N}\gamma_r R_r\frac{N}{\Delta\nu_{eff}}\right]+\sigma^2{}_{receiver}} . \quad (6)$$

Note, that for shot noise limited detection the sensitivity is independent of the number of pixels whereas it is not for receiver noise limited detection.

The sensitivity of TDOCT on the other hand reads

$$\Sigma_{TDOCT} = \frac{1}{B}\frac{2S^2\gamma_s\gamma_r P_0^2 R_R}{SP_0\gamma_r R_R\left(2q+SP_0\gamma_r R_R\frac{1+\Pi^2}{\Delta\nu_{eff}}\right)+(NEC)^2} . \quad (7)$$

In order to properly compare the sensitivities of both domains, we need to link the exposure time to the optimal bandwidth *B*. Following Rollins et al.[11] , using relation Eq. (3) and taking into account that the FDOCT scanning range amounts to *N/2* DFT bins, we obtain:

$$B = \frac{2v_g}{l_c} = \frac{2}{l_c}\frac{(scanning\ range)}{\tau} = \frac{N}{\Delta\tau^{(h)}_{FWHM}}\frac{1}{2\tau} = \frac{\pi}{4\ln 4}\frac{N}{m}\frac{1}{\tau}, \quad (8)$$

with group velocity v_g.

There are some effects due to the DFT which are characteristic for FD systems: Firstly, the detector of the spectrometer has a finite pixel width. Therefore we observe in fact the convolution of a rect function, corresponding to the pixel size, with the interferometer signal in the frequency domain. According to the convolution theorem the amplitude in the associated time domain is multiplied by a sinc function as shown in Fig. 1.

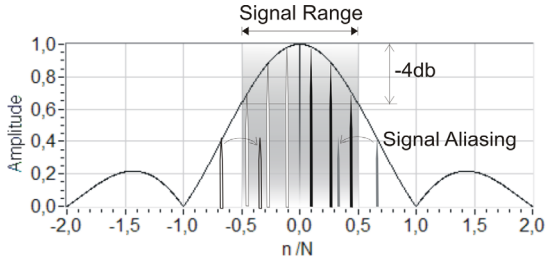

Fig. 1. FDOCT Signal amplitudes for various optical depths after Fourier transform.

Secondly, since we perform the DFT of a real function, the result will always be an even function. Each signal peak in the positive FFT range will have its mirror image in the negative frequency range (Fig. 1). The maximal depth position z_{max} corresponding to DFT bin N/2 is limited by the spectrometer resolution $\delta\lambda$ and is given by $z_{max} = \lambda^2/(4\delta\lambda)$. Any signal that exceeds this Nyquist limit will appear as aliased signal at DFT bin $N - n$ (Fig. 1). Also, the total noise power in the spectral domain is spread over all DFT bins in the time domain weighted by the sinc function. Noise frequencies outside the Nyquist border will however still be present within the signal range as aliased frequencies. This is why we assume a white noise characteristic, which, in case of photon noise, is associated with an average DC level of P_{ref}/N. The SNR will drop by ~ 4 dB as the signal peak approaches the Nyquist limit of *N/2*.

#2241 - $15.00 US Received March 17, 2003; Revised April 09, 2003

Different OCT realizations are shown in Fig. 2. A partially coherent light source is used with high spatial but low temporal coherence. The central part is usually a Michelson interferometer which splits the beam into a reference and sample arm signal. In the reference arm light is reflected back by a mirror, which is fixed in the case of FDOCT (Fig. 2 (a). For TDOCT the optical path length change of the reference arm provides the depth scanning. This is either done by a simple translation stage or by a rapid scanning optical delay line (RSOD). At the exit of the interferometer we have a PIN diode or a spectrometer with a detector array, for the respective OCT setups.

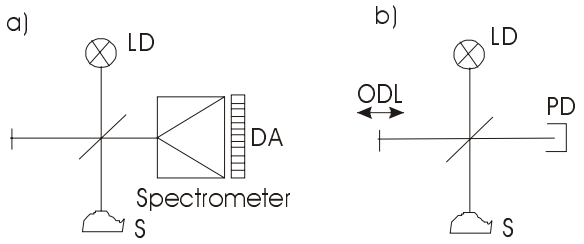

Fig. 2. Different OCT setups, with Optical Delay Line ODL, light source LD, photodiode PD, sample S, detector array DA. a) FDOCT, b) TDOCT.

In order to check the FDOCT noise model, we used the setup of Fig. 2(a). The light source was a superluminescent diode (λ_0= 811nm, *FWHM*=17nm, P_0=175µW, 60µW at the sample), the array detector was an ANDOR CCD camera with 1024 horizontal pixels. The spectrometer imaged the FWHM onto 470 CCD pixels. We used an exposure time of τ = 1ms, which corresponds to an A-scan rate of 1000 scans per second. In order to obtain the frequency depending interference signal from the recorded wavelength depending pattern, we applied a software scaling algorithm before DFT. In addition we performed a subtraction of the reference arm signal, which was recorded initially by blocking the sample arm.

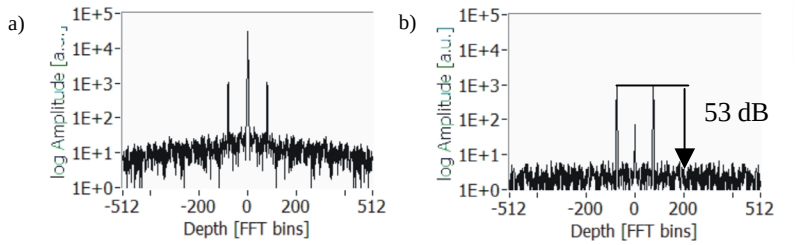

Fig. 3. a) FDOCT signal of a mirror and filter D=2 in the sample arm. b) The same signal with reference arm signal subtraction. The remaining DC peak in the center is due to the sample arm DC power.

The sensitivity was measured by first attenuating the reference arm signal such that the spectrum at the CCD was close to the saturation value. We then put a neutral density filter with D=2 into the sample arm. The sensitivity was calculated by measuring the SNR between signal peak after DFT and the ambient noise rms and adding 20 *D* = 40dB to this value. Fig. 3b shows a typical A-scan obtained with this configuration. The scan confirms nicely the assumed white noise characteristic for our noise model. The receiver noise for the CCD at room temperature was measured to 250 electrons per read out cycle and pixel.

In order to compare the theory with our experimental results we took the actual values of our experimental setup and compared it with the FDOCT noise model and to ideal time domain setups with 50/50 splitting ratio. The results are shown in Fig. 4 below.

#2241 - $15.00 US Received March 17, 2003; Revised April 09, 2003

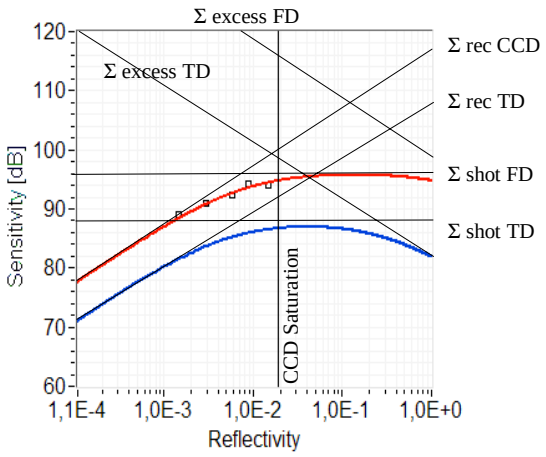

Fig. 4. The red line shows the theoretical sensitivity for FDOCT according to Eq. (6) with γ_r=0.15, γ_s=0.07, ρ=0.19, η =0.4, P_0=175μW,τ=1ms, σ_{CCD}=250e^-(at room temperature), FWC=400 ke^- The blue line is the TDOCT sensitivity for an unbalanced configuration, with γ_r=γ_s =0.25, B=113 kHz, NEC=0,5pA/√Hz. The squared dots are the actual measured system sensitivities for our FDOCT system.

We immediately observe the better sensitivity of FDOCT systems as compared to TDOCT setups. The calculated curve coincides very well with the measured values for the system sensitivity (squared dots in Fig. 4). Moreover, we recognize that in the case of FDOCT excess noise is negligible as compared to receiver and shot noise. Hence, balanced detection would not improve the sensitivity remarkably as it did in TDOCT.

The question is, why this sensitivity advantage has not shown up in FDOCT tomograms so far. There is first the strong sensitivity to phase fluctuations during the exposure time, which causes blurring and averaging of the modulation depth on the array detector. This may be avoided by minimizing the exposure time to 1ms and below. Another important fact is the appearance of coherent noise terms caused by internal sample reflections and reflections on optical components in either interferometer arm as well as the high DC level. If the reference arm power is much higher than that of the sample arm, we can easily remove the coherent noise terms by subtracting the reference arm signal before performing the DFT[4] (see Fig. 3). For highly reflecting samples it will be necessary to apply phase shifting methods[12] that allow the complete removal of the coherent noise terms together with the DC peak.

We believe that FDOCT is the method of choice for situations for low light situations such as in high speed imaging. Of course one is not able to perform dynamic focussing. Still, it has the potential to monitor fast dynamic physiologic processes.

Acknowledgments

We like to acknowledge the Austrian National Bank (Jubilaeumsfonds grant Nr. 9654) for the financial support.